NIR Variability of obscured and unobscured X-ray sources in the COSMOS field

Paula Sánchez[1]; Paulina Lira[1]; Regis Cartier[2], Patricia Arevalo[3], UltraVISTA team
[1]Universidad de Chile, [2]University of Southampton, [3]Universidad de Valparaiso.

Abstract

AGNs are characterized by their time-variable continuum flux in every waveband in which they have been studied. However very little is known about their variability in the infrared. This waveband gives us information about the dust surrounding the accretion disk at low redshift, and about the accretion disk at high redshift. In this work, I present our statistical study of the NIR variability of AGNs in the COSMOS field, using UltraVISTA data. This dataset give us a huge sample of light curves, making possible to have a global description of the nature of AGNs for different ranges of redshift, and for different levels of obscuration, from which we can have a better understanding of the difference between type 1 and type 2 AGNs.

Introduction

Active galactic nuclei (AGN) are one of the most energetic phenomena in the universe, and are characterized by their time-variable flux. The characteristic time scale of the variability ranges from days to years, and it is strong at the X-ray, UV and optical ranges.

One of the most accepted models to explain the behavior of different types of AGN is the unified model. It postulate that a dusty torus around the central engine, is the responsible for the different classes of AGNs, which occur when we observe the source at different angles (Antonucci & Miller 1985), as can be seen in Figure 1. Since the dust mostly emits in the infrared region, we might expect that the variability observed in the near infrared region (NIR) come from two components, the accretion disk and the hottest part of the dusty torus.
Some authors propose that the transition between the two components occurs at λ~1μm. This has been seen both photometrically and spectroscopically (Figure 2) (Glass 1992, Landt et al. 2011).

Using the UltraVISTA data set we will analyze the NIR variability of the two classes of AGNs, in order to understand their differences, and also to test whether most sources show a transition between the disk and the torus emission at λ~1μm.

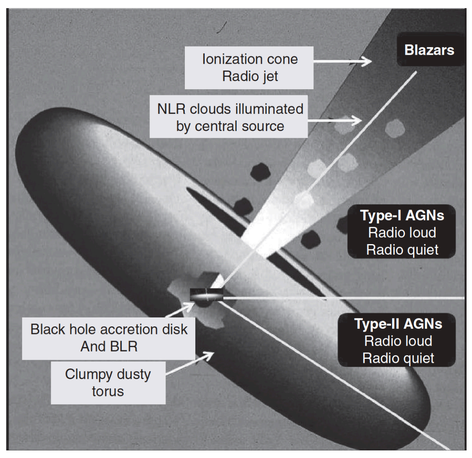

Figure 1. AGN types. Figure 6.9, Chapter 6, The Physics and Evolution of Active Galactic Nuclei, Hagai Netzer. Cambridge University Press, 2013.

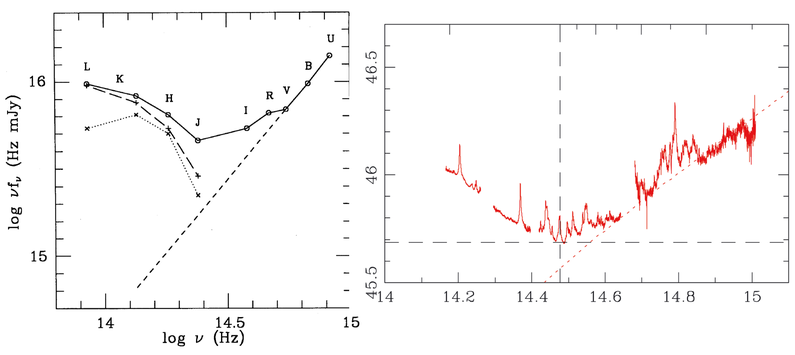

Figure 2. Photometric (left: Glass 1992) and spectroscopic (right: Landt et al. 2011) evidence of the transition between the disk and the torus (Glass 1992)

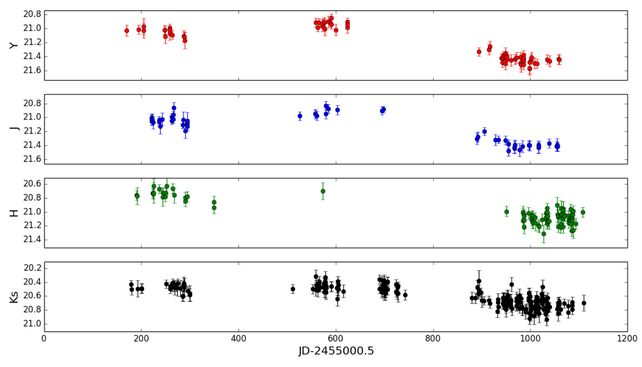

Figure 3. Light curve example. XMMC 149.46288+2.35668

Data

Our work is based on the YJHKs NIR imaging data from UltraVISTA (McCracken et al. 2012), a survey of the COSMOS field which covers an area of 1.5deg^2 . The data were taken between December 2009 and June 2012, with the VIRCAM instrument on the VISTA telescope at Paranal.

We worked with the individual images pre-processed by the Cambridge Astronomy Survey Unit (CASU), provided by the survey team, from which we have constructed our light curves (see Figure 3).

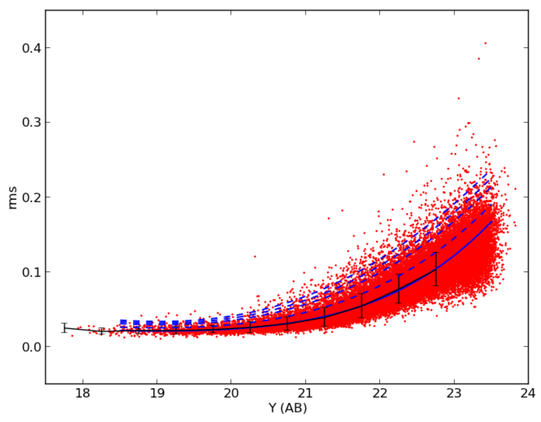

Figure 4. *Red dots:* Light curves standard deviation (std) vs mean magnitude for the filter Y. *Black line:* Values of the median std in bins of 0.5 magnitudes .*Blue line:* Fourth-degree polynomial model of the median std. *Dashed blue lines:* Fourth-degree polynomial models of the deviation of the median in 1, 2, 2.5 and 3σ

Methodology

In order to analyze known AGNs, we used the optical counterpart catalogs of the COSMOS field (Chandra COSMOS Survey, Civano et al. 2015; XMM-COSMOS survey, Brusa et al. 2010), and we constructed light curves for all objects with an AGN spectroscopic classification, that are detectable in our data set in at least 12 epochs and in a range of 200 rest frame days. Besides, we constructed light curves for all the objects of the UltraVISTA catalog (McCracken et al. 2012), to test the photometric errors of our data. For every light curve we measured the mean, median, and rms scatter.

Following the same approach of Sesar et al.(2007), we modeled the mean photometric error in function of the magnitude by fitting a fourth-degree polynomial to the median and standard deviation (σ) of the rms scatter (rms) of the light curves in 0.5 magnitude wide bins. Figure 4 shows the mean magnitude vs the rms for this sample in the filter Y, plus the model for the median and the 1, 2, 2.5 and 3σ deviations. From the Figure it is clear that brighter objects have lower photometric errors than weaker objects.

Using the models for the photometric errors in each filter, we can determine which objects are variable. From Figure 4, we can see that most of the objects are located below the 3σ curve. Other works in the optical range (e.g. De Cicco et al. 2014, Sesar et al. 2007), propose that objects above the 3σ curve are mostly variable. Given our larger photometric errors in the NIR regime we tested the method, by classifying objects as variable if they were above the 2, 2.5 and 3σ curves. In Table 1 we resume the results for all the filters. After a visual inspection of the light curves classified as variables, we decided to keep the 2.5σ criteria.

Filter	Total	2σ %	2.5σ %	3σ %
Y	246	13.0	10.2	6.9
J	261	13.8	8.8	6.5
H	304	6.9	4.9	3.3
Ks	290	7.9	5.2	3.8

Table 1. For each filter: Total number of detected AGNs, and the percentage of variable AGNs detected above 2, 2.5 and 3σ.

Results

Figure 5 gives the distribution of the absolute magnitude for the Ks filter as a function of redshift. To test the transition between the disk and the torus emission at λ~1μm, for every filter, we separate the sources by redshift in two groups: 1) sources at $z \le z_0$, and 2) sources at $z > z_0$, where z_0 is the redshift at which every filter is observing at rest-frame λ=1μm (z_0(Y,J,H,KS)=0.02,0.25,0.635,1.15). Charts 1 and 2 give the results.

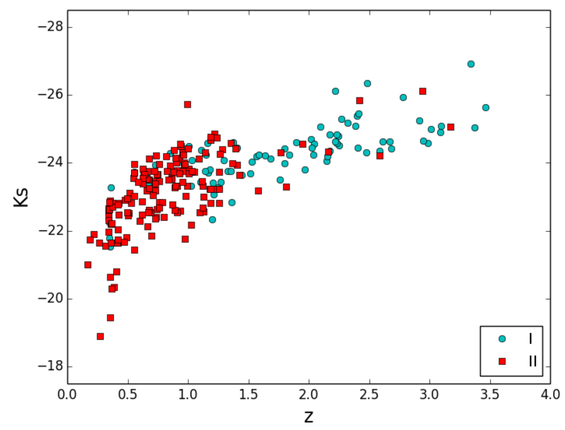

Figure 5. Absolute magnitude distribution in function of redshift

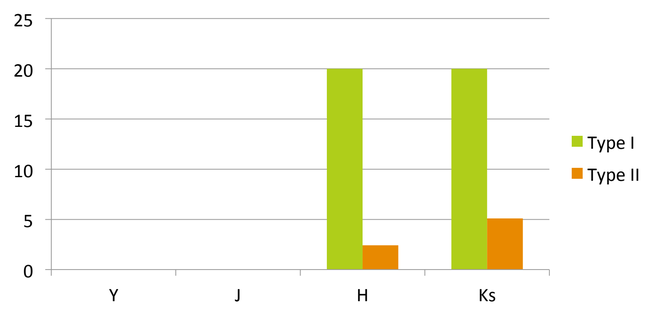

Chart 1. Percentage of variable objects for sources at $z \le z_0$

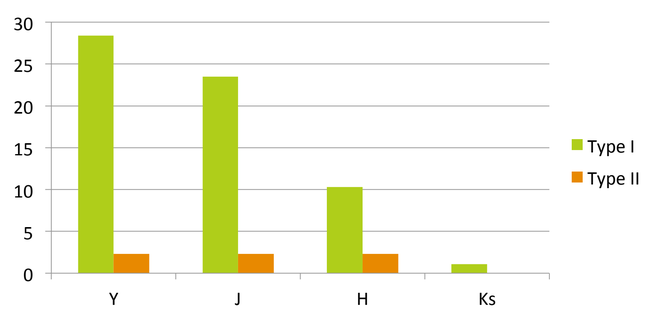

Chart 2. Percentage of variable objects for sources at $z > z_0$

Conclusions

- In Table 1 we can see that the percentage of variable objects is higher for the Y and J filter bands.
- From Charts 1 and 2, it is evident that the fraction of type I variable objects is much higher in both redshift ranges. Which was expected for $z > z_0$ (when looking at the disk), but not for $z < z_0$ (when looking at the torus).
- There is no clear evidence of the transition at λ~1μm. Which might cast doubts on the presence of a dusty torus in high-z sources.
- New methods to select variable objects are needed to be implemented, in order to get more clear and robust results.

Poster Template Designed by Genigraphics ©2012
1.800.790.4001 www.genigraphics.com